

## Thermal Studies of Aqueous Free-base Porphyrin and Metalloporphyrins of Trivalent and Tetravalent Metal Ions

S.D. GOKAKAKAR<sup>1,\*</sup> and A.V. SALKER<sup>2</sup>

<sup>1</sup>P.E.S.'s R.S.N. College of Arts and Science, Farmagudi, Ponda-403401, India

<sup>2</sup>School of Chemical Sciences, Goa University, Goa-403206, India

\*Corresponding author: E-mail: [sdgokakakar@gmail.com](mailto:sdgokakakar@gmail.com)

Received: 21 January 2022;

Accepted: 7 April 2022;

Published online: 18 July 2022;

AJC-20885

The free-base porphyrin and metalloporphyrins of Fe (monomer), Fe (dimer) and Sn (tin) were synthesized and purified by dry column chromatography. Aqueous free-base porphyrin and metalloporphyrins were characterized by UV-visible spectroscopy, IR spectroscopy and high-resolution mass spectrometry. Further, these synthesized porphyrins were subjected to TG-DSC analysis from room temperature to 800 °C. It was observed that each porphyrin has a characteristic first decomposition temperature and their thermal stabilities varied from 360-432 °C. Since, these aqueous porphyrins are highly hygroscopic in nature, their number of waters of crystallization were determined.

**Keywords:** Aqueous-porphyrins, Differential scanning calorimetry, Thermogravimetry, Residue analysis, Water of crystallization.

### INTRODUCTION

The structural studies of the porphyrin molecules have revealed that four pyrrole rings have joined together with four methine bridges to give a macrocyclic planar structure. It is an extended conjugated 18  $\pi$ -electron system makes it an aromatic molecule. Further, it has a cavity at the centre, which allows insertion of several metals and is the basis of the different metalloporphyrins [1,2]. A free-base porphyrin (*e.g.* TPPS<sub>4</sub>) can form chelate with various metal cations and exhibit the conformations such as planar, ruffled, domed or saddled, *etc.* It is also observed that depending upon the size of the metal ion there are two types of porphyrins. If the metal cation is having a size of 55-80 pm then in-plane metalloporphyrins are formed, where the metal centres are situated in the plane of porphyrin ring. In addition to the size of the metal ion other affecting factors are axial ligands or the size of the peripheral substituents, whereby, they can give rise to the typical distorted geometries. If the metal ion is having the size greater than 80-90 pm, then out-of-plane or sitting atop (SAT) metalloporphyrins are formed, where the metal ions are situated out of the plane of porphyrin ring [2,3].

The synthetic porphyrins are the promising candidates for treatment of diseases [4], industries [5], biological imaging [6],

analytical purposes [7], photocatalytic heterogeneous catalysis [8-12], non-linear optics [13] and molecular photovoltaics [14, 15]. Further, in the recent past, the applications of porphyrins are extended in the fields of single cell imaging [16-18], drug delivery, chemosensors [19], MRI and photodynamic cancer therapy (PDT), *etc.* Advanced researchers have prepared broad-spectrum porphyrins which are also known as texaphyrins and their metal complexes for potential applications in magnetic resonance imaging, where imaging relating modalities such as magnetic resonance imaging (MRI), position imaging tomography (PIT), photoacoustic tomography (PAT), fluorescence imaging (FI), ultrasonography and X-ray radiography are involved [20-22].

It is to be noted that in chemical industries, around 80% of the chemical transformations are carried out by catalysis [23,24]. It is also an evidenced fact that in the past decades, nanocatalysts have gained the utter importance due to their size effect [25]. Therefore, reducing the particle size was specially emphasized to boost better catalytic activity, where, the attempts were done to make the catalyst to atomic size dimension [26]. Thus, with the advent and advancement of aberration-corrected transmission electron microscope (AC-TEM) and X-ray adsorption fine spectra (XAFS), the characterization of catalysts at atomic level was possible. It was also observed that when the

size of the particle gets reduced to the atomic level, it shows distinct and unique catalytic properties from nanoparticles.

The natural metalloporphyrins such as haemoglobin used in oxygen transportation or chloroplast required in photosynthesis are long known. Exploring the idea of biomimetics, applications of porphyrins are extended to many catalytic reactions, *viz.* electrocatalytic oxygen reduction reactions (ORR), epoxidation of olefins, oxidation of alkanes and coupling reactions [27-31].

The objective of present study is to focus on the thermal stabilities of TPPS<sub>4</sub>, FeTPPS<sub>4</sub>Cl, (FeTPPS<sub>4</sub>)<sub>2</sub>-O and SnTPPS<sub>4</sub>Cl<sub>2</sub>, which are used for variety of reactions in chemistry, diagnostic therapies, homogeneous and heterogeneous catalytic reactions. All the respective porphyrins were subjected to the thermal analysis for the fixation of water of crystallization molecules, their all-decomposition temperatures in synthetic air medium, qualitative and quantitative analysis for the presence of %Na<sup>+</sup>, %SO<sub>4</sub><sup>2-</sup>, %M of respective metal oxide (in case of metalloporphyrins), % of carbon, *etc.*

## EXPERIMENTAL

A free-base porphyrin, tetrasodium *meso*-tetra(*p*-sulphonatophenyl)porphyrin (TPPS<sub>4</sub>), was synthesized by using vacuum dried tetraphenyl porphyrin (TPP) and conc. H<sub>2</sub>SO<sub>4</sub> in the molar ratio 0.003:0.5. The reaction mixture was refluxed for about 8 h and allowed to stand for 48 h undisturbed. Further, the lime and distilled water were added to the assembly to get purple colour. At this stage the byproduct CaSO<sub>4</sub> was removed, the pH of the solution was adjusted to 8-10 by the addition of Na<sub>2</sub>CO<sub>3</sub>. The precipitate of CaCO<sub>3</sub> was removed followed by addition of ethyl alcohol as requirement. The filtrate was dried in oven at 100 °C for continuous 2 h to get purple coloured deliquescent crystals of TPPS<sub>4</sub>. The dry column chromatography was used to purify the product. The stationary phase was employed as basic alumina and the mobile phase was prepared by addition of water, methanol and acetone in the ratio 7:2:1. During purification, only purple band (TPPS<sub>4</sub>) was selected and remaining green band due to dication was rejected. After purification, the product, TPPS<sub>4</sub> was vacuum dried and preserved in air-tight container for subsequent synthesis of metalloporphyrins [32].

The synthesis of metalloporphyrins was carried out by introducing the metals such as Fe and Sn into the free-base porphyrin hole. Trivalent metal porphyrins such as FeTPPS<sub>4</sub>Cl and its dimer [O-(FeTPPS<sub>4</sub>)<sub>2</sub>] were synthesized by using the reported method [33] with the modification, where the metal salt was added in excess than stoichiometric proportion required. The difficulty was in the synthesis where, 10-fold excess salt of tetravalent Sn was required to get the formation of SnTPPS<sub>4</sub>Cl<sub>2</sub>. For purification of above synthesized porphyrins, dry column chromatography was used, where green band due to dication [H<sub>4</sub>(TPPS<sub>4</sub>)<sup>2+</sup>] and colourless band due to unreacted excess salt were rejected. Thus, the appropriate band due to a specific metalloporphyrin was selected, tested for purity using TLC, concentrated, vacuum dried, placed in an air tight container and were used in subsequent operations.

The characteristic absorption bands in UV and visible regions were recorded using Shimadzu spectrophotometer (model UV/2450UV). The infrared spectra of these porphyrins were recorded on Shimadzu spectrometer (model prestige/21FTIR). The mass of the specific metalloporphyrin was determined using High-resolution mass spectrometer using (model Varian 500-MS). The TG-DSC analysis of the above compounds was carried out on NETZSCH-Geratbau GmbH thermal analyser (STA 409PC) from room temperature to 800 °C.

## RESULTS AND DISCUSSION

**UV-visible studies:** The porphyrins as synthesized above *viz.* TPPS<sub>4</sub>, FeTPPS<sub>4</sub>Cl, (FeTPPS<sub>4</sub>)<sub>2</sub>-O and SnTPPS<sub>4</sub>Cl<sub>2</sub> were characterized by UV-visible spectroscopy with reference to their characteristic bands in visible and Soret region as shown in Figs. 1 and 2. It is observed that as a representative porphyrin for (FeTPPS<sub>4</sub>)<sub>2</sub>-O, the two different concentrations *i.e.* 10<sup>-4</sup> M and 10<sup>-5</sup> M were used. For higher concentration, the resolution of peaks was not observed whereas for the lower concentration (10<sup>-5</sup> M), the peaks are clearly seen. In soret region, it was observed that depending upon the respective porphyrin, the absorption bands were 413 nm (TPPS<sub>4</sub>), 394 nm (FeTPPS<sub>4</sub>Cl), 395 nm (FeTPPS<sub>4</sub>)<sub>2</sub>-O and 418 nm (SnTPPS<sub>4</sub>Cl<sub>2</sub>), respectively [33,34].

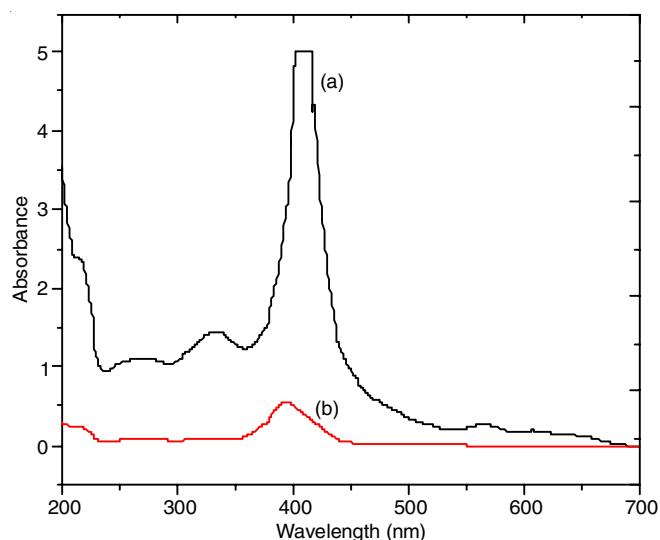


Fig. 1. UV-visible spectra of (FeTPPS<sub>4</sub>)<sub>2</sub>-O (a) 10<sup>-4</sup> M concentration, (b) 10<sup>-5</sup> M concentration

**FTIR studies:** In sulphonated porphyrins, the key characteristic bands are the confirmation of substitution of SO<sub>3</sub>Na group at four *para*-positions in phenyl rings of tetraphenyl porphyrin molecule. These bands in TPPS<sub>4</sub> were 1041, 1128 and 1184 cm<sup>-1</sup>, for FeTPPS<sub>4</sub>Cl: 1240-1175, 1130 and 1141 cm<sup>-1</sup>, for (FeTPPS<sub>4</sub>)<sub>2</sub>-O: 1188, 1128 and 1041 cm<sup>-1</sup>, for SnTPPS<sub>4</sub>Cl<sub>2</sub>: 1195, 1130 and 1041 cm<sup>-1</sup> respectively [33,34]. Further, it should be noted that the monomer FeTPPS<sub>4</sub>Cl and a dimer (FeTPPS<sub>4</sub>)<sub>2</sub>-O are distinguished from each other by 850 and 881 cm<sup>-1</sup> bands due to Fe-O-Fe stretching in dimer (Fig. 3).

**High resolution mass studies:** As a representative compound of porphyrins, FeTPPS<sub>4</sub>Cl was subjected to high resolution

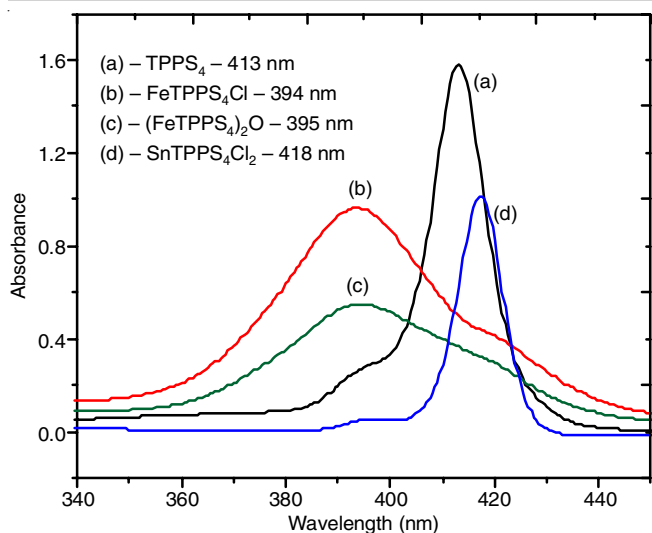
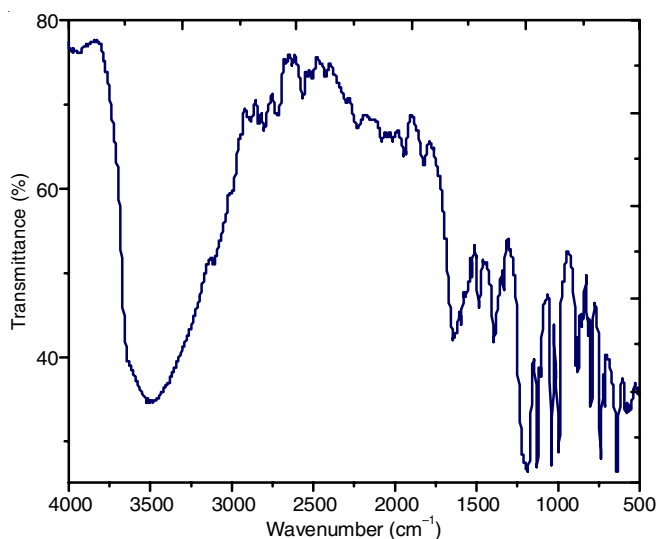
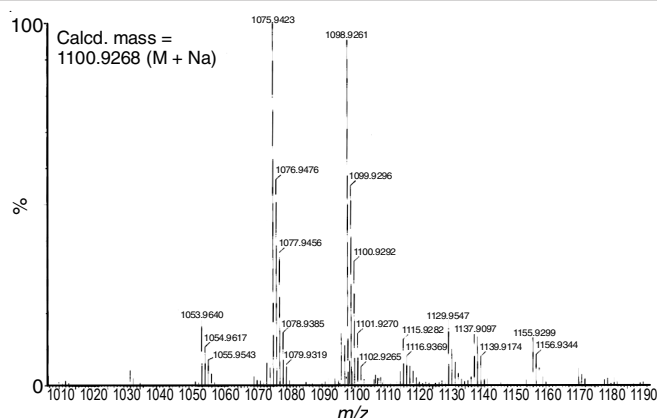
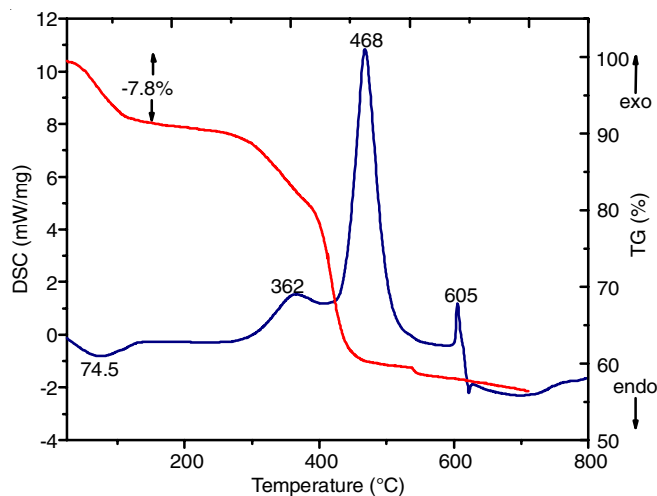


Fig. 2. Overlay of Soret bands in UV-visible region for selected porphyrins

Fig. 3. IR spectra of FeTPPS<sub>4</sub>Cl

mass spectrometry for the calculation of the molecular weight and it was confirmed as shown in Fig. 4.

**TG/DSC studies:** The TG and DSC analytical methods revealed the various inferences, which were systematically recorded for all porphyrins under study from room temperature to 800 °C in synthetic air atmosphere. Fig. 5 shows TG/DSC curve for TPPS<sub>4</sub>. The compound is highly hygroscopic in nature therefore the endothermic peak at 74.5 °C is seen and it shows a weight loss of 7.8% due to water of crystallization. From this observation, the number of molecules of water of crystallization were confirmed as five and therefore, the molecular formula of a compound can be written as TPPS<sub>4</sub>·5H<sub>2</sub>O (Table-1). The

Fig. 4. High resolution mass spectra for molecular weight of FeTPPS<sub>4</sub>ClFig. 5. TG/DSC curve for free-base TPPS<sub>4</sub>

subsequent mass loss after loss of water molecules is observed at 360 °C, it is seen that compound starts decomposing which is shown by DSC curve (Fig. 5). The next decomposition temperatures are 468 and 605 °C, respectively. After the last decomposition temperature, the calculation shows that the TPPS<sub>4</sub> loses 44% of the total material and residue remaining is 56% (Table-2). The TG-DSC event clarifies that TPPS<sub>4</sub> decomposes in three stages and the thermal stability of a compound is up to around 360 °C.

**Analysis of residue of TPPS<sub>4</sub>:** The qualitative analysis of the residue of TPPS<sub>4</sub> has shown the presence of Na<sup>+</sup>, SO<sub>4</sub><sup>2-</sup> and a coal, which is a decomposition product of aromatic ring of porphyrin. The TG-DSC analysis confirmed that Na<sup>+</sup> ion is not lost during thermal analysis because its b.p. is 881 °C and our experimental limiting temperature is up to 800 °C. In the context of SO<sub>3</sub><sup>2-</sup> substituents on the phenyl rings, the TG-EGA-MS analysis [35] has shown that the loss of S<sup>+</sup>, HS<sup>+</sup>,

TABLE-1  
FIXATION OF WATER OF CRYSTALLIZATION MOLECULES IN AQUEOUS-PORPHYRINS

Porphyrin	Weight taken for TG-DSC (mg)	Loss due to H <sub>2</sub> O (%)	Molecular weight of anhydrous compound	Molar ratio	Number water of crystallization molecules	Formula
TPPS <sub>4</sub>	10.000	-7.80	1024	1:5	05	TPPS <sub>4</sub> ·5H <sub>2</sub> O
FeTPPS <sub>4</sub> Cl	11.700	-15.52	1115.25	1:11	11	FeTPPS <sub>4</sub> Cl·11H <sub>2</sub> O
(FeTPPS <sub>4</sub> ) <sub>2</sub> -O	12.600	-9.44	2177.7	1:13	13	(FeTPPS <sub>4</sub> ) <sub>2</sub> -O·13H <sub>2</sub> O
SnTPPS <sub>4</sub> Cl <sub>2</sub>	12.200	-2.86	1213.5	1:2	02	SnTPPS <sub>4</sub> Cl <sub>2</sub> ·2H <sub>2</sub> O

TABLE-2  
% TOTAL LOSS OF THE MATERIAL AND THE RESIDUE REMAINING DURING AND AFTER THE TG/DSC OPERATION

Porphyrin	Loss due to H <sub>2</sub> O (%)	Loss due to porphyrin (%)	Total loss (%)	Residue remaining (%)
TPPS <sub>4</sub>	-7.80	36.23	44	56
FeTPPS <sub>4</sub> Cl	-15.52	30.48	46	54
(FeTPPS <sub>4</sub> ) <sub>2</sub> -O	-9.44	35.56	45	55
SnTPPS <sub>4</sub> Cl <sub>2</sub>	-2.86	39.14	42	58

H<sub>2</sub>S species is observed. It is to be emphasized that the part of the sulphur from SO<sub>3</sub><sup>2-</sup> is lost in the form of above-mentioned species and remaining part of the SO<sub>3</sub><sup>2-</sup> group is oxidized to SO<sub>4</sub><sup>2-</sup> ions due to the synthetic air environment. This was confirmed by the necessary confirmative tests. Therefore, the residue of TPPS<sub>4</sub> after TG-DSC analysis has shown 8.97% Na<sup>+</sup>, 37.49% SO<sub>4</sub><sup>2-</sup> and 53.53% carbon (Table-3).

**TG/DSC of FeTPPS<sub>4</sub>Cl:** The TG/DSC curve for FeTPPS<sub>4</sub>Cl is shown in Fig. 6. The TG curve shows 15.52% loss due to water of crystallization at 80.8 °C. The molar ratio of the compound to water was calculated as 1:11, therefore, the molecular formula of the compound can be written as FeTPPS<sub>4</sub>Cl·11H<sub>2</sub>O (Table-1). The loss due to porphyrin ring is 30.80% and hence it is evident that total loss in the compound including the loss due to water molecules during thermal analysis is 46% and the residue remaining is 54% (Table-2). The DSC curve for the

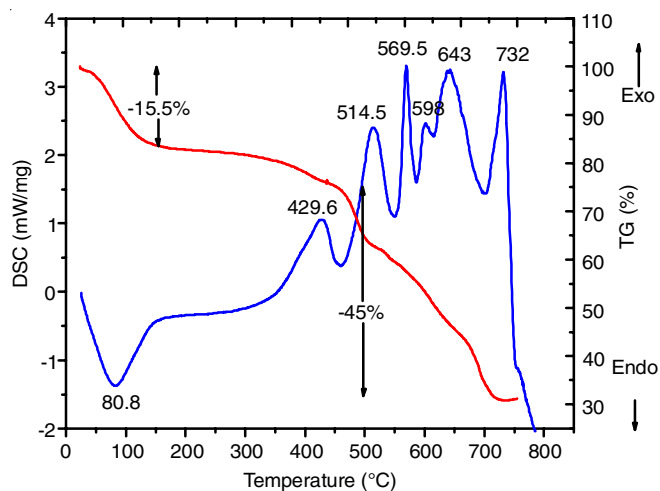


Fig. 6. TG/DSC curve for FeTPPS<sub>4</sub>Cl

compound shows six different decomposition temperatures at 429.6, 514.5, 569.5, 598, 643 and 732 °C. This indicates that the porphyrin FeTPPS<sub>4</sub>Cl is stable up to 429 °C.

**Analysis of residue of FeTPPS<sub>4</sub>Cl:** The residue of the above compound was analyzed after the completion of TG-DSC operation at 800 °C. The results were obtained as 8.27% Na<sup>+</sup>, 34.43% SO<sub>4</sub><sup>2-</sup>, 45.65% carbon and 11.63% Fe<sub>2</sub>O<sub>3</sub> (Table-3). The magnetic studies of the compound revealed the a low-spin chelate. Since, synthetic air environment is used for the TG-DSC operation, which is highly oxidizing, the expected metal oxide is Fe<sub>2</sub>O<sub>3</sub>.

**TG/DSC of (FeTPPS<sub>4</sub>)<sub>2</sub>-O:** For (FeTPPS<sub>4</sub>)<sub>2</sub>-O (dimer of iron), the TG-DSC curve is shown in Fig. 7. The TG curve of a compound shows 9.44% loss due to water of crystallization at 92.7 °C. The corresponding molar ratio obtained for this compound was 1:13, therefore, the molecular formula for this metalloporphyrin can be given as (FeTPPS<sub>4</sub>)<sub>2</sub>-O·13H<sub>2</sub>O (Table-1). When loss due to porphyrin ring is taken into account it is 35.56% and total loss including water of crystallization is 45%, while the residue remaining is 55% (Table-2). The DSC curve for (FeTPPS<sub>4</sub>)<sub>2</sub>-O shows that the compound decomposes in four different stages at 432, 524.4, 573 and 696 °C, respectively.

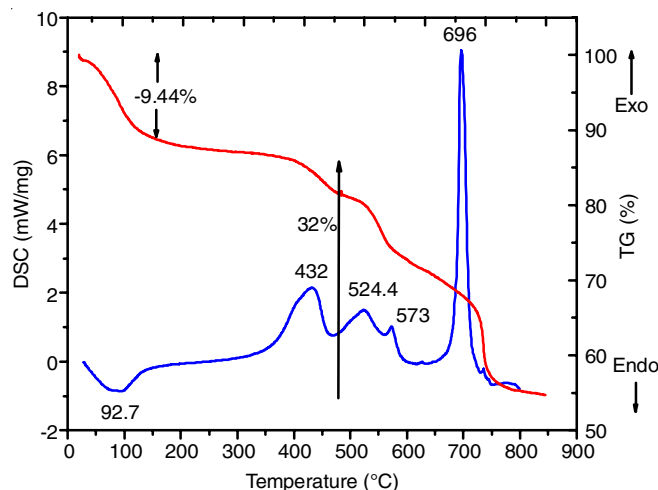


Fig. 7. TG/DSC curve for (FeTPPS<sub>4</sub>)<sub>2</sub>-O

**Analysis of residue of (FeTPPS<sub>4</sub>)<sub>2</sub>-O:** The residue of the compound after TG-DSC analysis gave 4.23% Na<sup>+</sup>, 16.26% SO<sub>4</sub><sup>2-</sup>, 67.60% coal and 11.90% Fe<sub>2</sub>O<sub>3</sub> (Table-3). The magnetic

TABLE-3  
QUANTITATIVE ANALYSIS OF RESIDUE OF PORPHYRINS BASED ON TG-DSC MEASUREMENTS

Porphyrin	TPPS <sub>4</sub>	FeTPPS <sub>4</sub> Cl	(FeTPPS <sub>4</sub> ) <sub>2</sub> -O	SnTPPS <sub>4</sub> Cl <sub>2</sub>
Wt. of porphyrin taken (mg)	9.40	11.70	12.60	12.20
Residue remaining (mg)	5.26	3.63	6.93	10.00
Residue loss (mg)	4.14	8.07	5.67	2.20
Amount of Na <sup>+</sup> (mg)	0.47	0.30	0.29	0.76
Na <sup>+</sup> (%)	8.97	8.27	4.23	7.58
Amount of SO <sub>4</sub> <sup>2-</sup> (mg)	1.97	1.25	1.13	3.16
SO <sub>4</sub> <sup>2-</sup> (%)	37.49	34.43	16.26	31.64
Amount of metal oxide (mg)	–	0.42	0.82	1.24
Metal oxide (%)	–	11.63	11.90	12.41
Amount of coal	2.82	1.66	4.68	4.84
Coal (%)	53.53	45.65	67.60	48.42

measurement has shown that it is a low spin paramagnetic chelate and its final chemical composition as a metal oxide expected is  $\text{Fe}_2\text{O}_3$  as a most stable oxide of Fe.

**TG/DSC of  $\text{SnTPPS}_4\text{Cl}_2$ :** Fig. 8 shows TG-DSC curve for  $\text{SnTPPS}_4\text{Cl}_2$ . The TG curve shows 2.86% loss at 60.6 °C due to water of crystallization. The respective molar ratio obtained for this was 1:2, therefore, the molecular formula can be elucidated as  $\text{SnTPPS}_4\text{Cl}_2 \cdot 2\text{H}_2\text{O}$  (Table-1). It is also seen that the loss due to porphyrin material as shown by TG curve is around 39.14% and therefore, total loss sums up to 42% and the residue remaining is 58% (Table-2). The DSC curve for  $\text{SnTPPS}_4\text{Cl}_2$  shows three decomposition temperatures as 409, 458 and 563 °C, respectively.

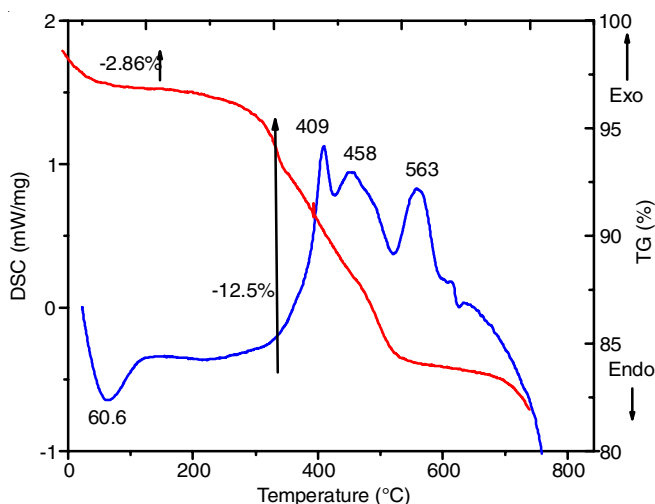


Fig. 8. TG/DSC curve for  $\text{SnTPPS}_4\text{Cl}_2$

**Analysis of residue of  $\text{SnTPPS}_4\text{Cl}_2$ :** The residue of the compound after TG-DSC analysis gave 7.58%  $\text{Na}^+$ , 31.64%  $\text{SO}_4^{2-}$ , 48.42% coal and 12.41%  $\text{SnO}_2$  (Table-3). The magnetic measurement has shown that it is a diamagnetic chelate and its final chemical composition as a metal oxide is expected as  $\text{SnO}_2$  as a most stable oxide of Sn.

**First decomposition temperature and relative thermal stabilities of porphyrins:** The information of first decomposition temperature of a respective porphyrin confirms the thermal stability of the corresponding porphyrin, which can be used for any suitable applications (Fig. 9). Similarly, the total loss brought about due to exclusive porphyrin ring is shown by thermogravimetric curves in Fig. 10. With regards to the observation, it is seen that  $(\text{FeTPPS}_4)_2\text{O}$  is the most thermally stable metalloporphyrin. In the structure of this compound, two porphyrin rings are joined together with a bridge of oxygen to two  $\text{Fe}^{3+}$  ions, where slightly more energy would be required to rupture two O-porphyrin bonds. In case of  $\text{FeTPPS}_4\text{Cl}$ , first there is a removal of axial Cl ligand and then subsequently fragmentation of porphyrin ring is followed, which will be having more or less same thermal stability as of the dimer due to loosely bonded Cl and strongly bonded Fe-N in the core of the porphyrin. For  $\text{SnTPPS}_4\text{Cl}_2$ , there are two axial Cl ligands, one above and another below the square plane. It may be expected that when both the similar ligands are simultaneously

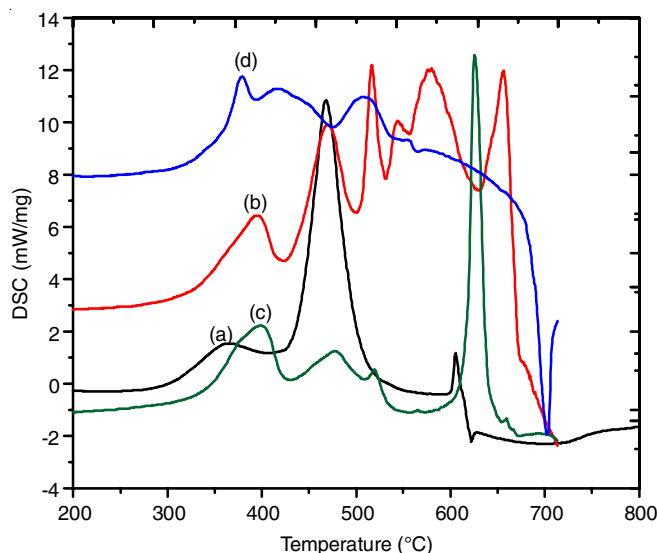


Fig. 9. First decomposition temperature of each selected porphyrin, (a)  $\text{TPPS}_4$  - 361 °C, (b)  $\text{FeTPPS}_4\text{Cl}$  - 429.6 °C, (c)  $(\text{FeTPPS}_4)_2\text{O}$  - 432 °C, (d)  $\text{SnTPPS}_4\text{Cl}_2$  - 409 °C

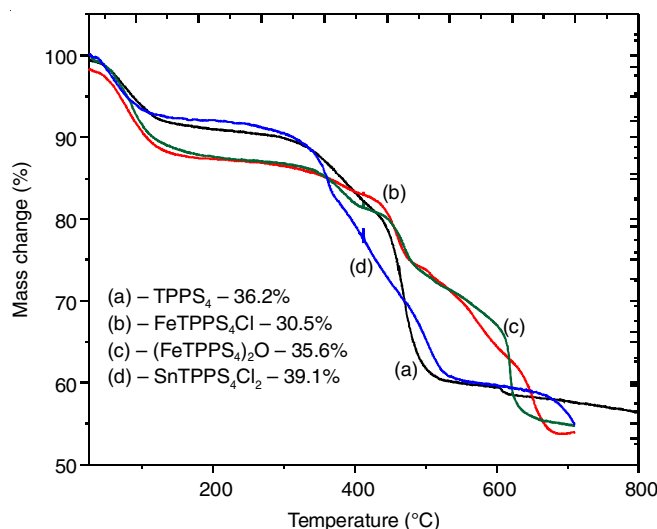


Fig. 10. Loss of exclusive porphyrin during TG measurements

removed in the thermal event, would be causing the instability in the structure to decompose at the lower temperature of 409 °C as compared to above metalloporphyrins. In  $\text{TPPS}_4$ , which is a free-base porphyrin has no metal but two N-H bonds in the core of the porphyrin ring. Due to these stretching vibrations, the compound is comparatively less stable as compared with the preceding porphyrins and cleavage of the bonds would be commencing from the pyrrole rings and then opening up of the phenyl rings. Therefore,  $\text{TPPS}_4$  shows comparatively least thermal stability among the selected porphyrins. Hence, the order of thermal stability for the above porphyrins can be given as:



## Conclusion

The precursor tetrasodium *meso*-tetra(*p*-sulphonatophenyl)-porphyrin ( $\text{TPPS}_4$ ), a free-base porphyrin was used for the synthesis of metalloporphyrins *e.g.*  $\text{FeTPPS}_4\text{Cl}$ ,  $\text{SnTPPS}_4\text{Cl}_2$ ,

(FeTPPS<sub>4</sub>)<sub>2</sub>-O and characterized by the standard established methods. These aqueous- porphyrins were highly hygroscopic in nature, therefore, the number of molecules of water of crystallization were calculated for each porphyrin as TPPS<sub>4</sub>·5H<sub>2</sub>O, FeTPPS<sub>4</sub>Cl·11H<sub>2</sub>O, (FeTPPS<sub>4</sub>)<sub>2</sub>-O·13H<sub>2</sub>O and SnTPPS<sub>4</sub>Cl<sub>2</sub>·2H<sub>2</sub>O. The TG-DSC measurements were used to determine the total loss of the porphyrin, the amount of residue remaining after operation and the first and subsequent decomposition temperatures. The remaining residues after the TG-DSC operation was used to determine the %Na<sup>+</sup>, %SO<sub>4</sub><sup>2-</sup>, % carbon and % of respective metal oxide in case of metalloporphyrins.

### ACKNOWLEDGEMENTS

The authors are grateful to UGC, New Delhi for providing the minor financial support to this investigation.

### CONFLICT OF INTEREST

The authors declare that there is no conflict of interests regarding the publication of this article.

### REFERENCES

- A.M. Santoro, M.C. Lo Giudice, A. D'Urso, R. Lauceri, R. Purrello and D. Milardi, *J. Am. Chem. Soc.*, **134**, 10451 (2012); <https://doi.org/10.1021/ja300781u>
- Z. Valicsek and O. Horváth, *Microchem. J.*, **107**, 47 (2013); <https://doi.org/10.1016/j.microc.2012.07.002>
- Z. Valicsek, G. Eller and O. Horváth, *Dalton Trans.*, **41**, 13120 (2012); <https://doi.org/10.1039/c2dt31189e>
- A.A. Ptaszynska, M. Trytek, G. Borsuk, K. Buczek, K. Rybicka-Jasinska and D. Gryko, *Sci. Rep.*, **8**, 5523 (2018); <https://doi.org/10.1038/s41598-018-23678-8>
- P. Zucca, C. Neves, M.M. Simões, M. Neves, G. Cocco and E. Sanjust, *Molecules*, **21**, 964 (2016); <https://doi.org/10.3390/molecules21070964>
- G. Varchi, F. Foglietta, R. Canaparo, M. Ballestri, F. Arena, G. Sotgiu, A. Guerrini, C. Nanni, G. Cicoria, G. Cravotto, S. Fanti and L. Serpe, *Nanomedicine*, **10**, 3483 (2015); <https://doi.org/10.2217/nnm.15.150>
- M. Biesaga, *Talanta*, **51**, 209 (2000); [https://doi.org/10.1016/S0039-9140\(99\)00291-X](https://doi.org/10.1016/S0039-9140(99)00291-X)
- R.C. e Silva, L.O. da Silva, A. de Andrade Bartolomeu, T.J. Brocksom and K.T. de Oliveira, *Beilstein J. Org. Chem.*, **16**, 917 (2020); <https://doi.org/10.3762/bjoc.16.83>
- A.M. Huerta-Flores, G. Bengasi, K. Baba and N.D. Boscher, *ACS Appl. Energy Mater.*, **3**, 9848 (2020); <https://doi.org/10.1021/acsaem.0c01545>
- P.D. Harvey, *J. Mater. Chem. C*, **9**, 16885 (2021); <https://doi.org/10.1039/D1TC04147A>
- S.D. Gokakakar, P.A. Pavaskar and A.V. Salker, *SN Appl. Sci.*, **2**, 294 (2020); <https://doi.org/10.1007/s42452-020-1989-8>
- F. Leng, H. Liu, M. Ding, Q.P. Lin and H.L. Jiang, *ACS Catal.*, **8**, 4583 (2018); <https://doi.org/10.1021/acscatal.8b00764>
- D. Dini, M.J. Calvete and M. Hanack, *Chem. Rev.*, **116**, 13043 (2016); <https://doi.org/10.1021/acs.chemrev.6b00033>
- G. de la Torre, G. Bottari, M. Sekita, A. Hausmann, D.M. Guldi and T. Torres, *Chem. Soc. Rev.*, **42**, 8049 (2013); <https://doi.org/10.1039/c3cs60140d>
- S. Saito and A. Osuka, *Angew. Chem. Int. Ed.*, **50**, 4342 (2011); <https://doi.org/10.1002/anie.201003909>
- X. Dong, H. Chen, J. Qin, C. Wei, J. Liang, T. Liu, D. Kong and F. Lv, *Drug Deliv.*, **24**, 641 (2017); <https://doi.org/10.1080/10717544.2017.1289570>
- A.S. Stender, K. Marchuk, C. Liu, S. Sander, M.W. Meyer, E.A. Smith, B. Neupane, G. Wang, J. Li, J.-X. Cheng, B. Huang and N. Fang, *Chem. Rev.*, **113**, 2469 (2013); <https://doi.org/10.1021/cr300336e>
- C.M. Lemon, E. Karnas, X. Han, O.T. Bruns, T.J. Kempa, D. Fukumura, M.G. Bawendi, R.K. Jain, D.G. Duda and D.G. Nocera, *J. Am. Chem. Soc.*, **137**, 9832 (2015); <https://doi.org/10.1021/jacs.5b04765>
- H. Ali and J.E. van Lier, *Chem. Rev.*, **99**, 2379 (1999); <https://doi.org/10.1021/cr980439y>
- T. Jahanbin, H. Sauriat-Dorizon, P. Spearman, S. Benderbous and H. Korri-Youssoufi, *Mater. Sci. Eng. C*, **52**, 325 (2015); <https://doi.org/10.1016/j.msec.2015.03.007>
- E. Lancelot, *Invest. Radiol.*, **51**, 691 (2016); <https://doi.org/10.1097/RLI.0000000000000280>
- F. Chen, X.Z. Jiang, L.L. Zhang, R. Lang and B.T. Qiao, *Chin. J. Catal.*, **39**, 893 (2018); [https://doi.org/10.1016/S1872-2067\(18\)63047-5](https://doi.org/10.1016/S1872-2067(18)63047-5)
- S. Ji, Y. Chen, X. Wang, Z. Zhang, D. Wang and Y. Li, *Chem. Rev.*, **120**, 11900 (2020); <https://doi.org/10.1021/acs.chemrev.9b00818>
- L. Liu and A. Corma, *Chem. Rev.*, **118**, 4981 (2018); <https://doi.org/10.1021/acs.chemrev.7b00776>
- D. Gao, H. Zhou, J. Wang, S. Miao, F. Yang, G. Wang, J. Wang and X. Bao, *J. Am. Chem. Soc.*, **137**, 4288 (2015); <https://doi.org/10.1021/jacs.5b00046>
- H. Tang, H. Yin, J. Wang, N. Yang, D. Wang and Z. Tang, *Angew. Chem. Int. Ed.*, **52**, 5585 (2013); <https://doi.org/10.1002/anie.201300711>
- W. Zhang, W. Lai and R. Cao, *Chem. Rev.*, **117**, 3717 (2017); <https://doi.org/10.1021/acs.chemrev.6b00299>
- M.L. Merlau, M. del Pilar Mejia, S.B.T. Nguyen and J.T. Hupp, *Angew. Chem. Int. Ed.*, **40**, 4239 (2001); [https://doi.org/10.1002/1521-3773\(20011119\)40:22<4239::AID-ANIE4239>3.0.CO;2-E](https://doi.org/10.1002/1521-3773(20011119)40:22<4239::AID-ANIE4239>3.0.CO;2-E)
- C.M. Che, V.K. Lo, C.Y. Zhou and J.S. Huang, *Chem. Soc. Rev.*, **40**, 1950 (2011); <https://doi.org/10.1039/c0cs00142b>
- S.H. Cho, J.Y. Kim, J. Kwak and S. Chang, *Chem. Soc. Rev.*, **40**, 5068 (2011); <https://doi.org/10.1039/c1cs15082k>
- T.S. Srivastava and M. Tsutsui, *J. Org. Chem.*, **38**, 2103 (1973); <https://doi.org/10.1021/jo00951a036>
- E.B. Fleischer, J.M. Palmer, T.S. Srivastava and A. Chatterjee, *J. Am. Chem. Soc.*, **93**, 3162 (1971); <https://doi.org/10.1021/ja00742a012>
- W.D.W. Horrocks Jr, and E.G. Hove, *J. Am. Chem. Soc.*, **100**, 4386 (1978); <https://doi.org/10.1021/ja00482a012>
- F.R. Hopf and D.G. Whitten, Eds.: K.M. Smith, Porphyrins and Metalloporphyrins, Elsevier, Amsterdam, Chap. 16, pp. 667 (1975).
- S.D. Gokakakar and A.V. Salker, *J. Therm. Anal. Calorim.*, **109**, 1487 (2012); <https://doi.org/10.1007/s10973-011-1952-4>